

Numerical study of light correlations in a random medium close to the Anderson localization threshold

Shih-Hui Chang and Allen Taflove

Department of Electrical and Computer Engineering, Northwestern University, Evanston, Illinois 60208

Alexey Yamilov, Aleksander Burin, and Hui Cao

Department of Physics and Astronomy, Northwestern University, Evanston, Illinois 60208

Received October 28, 2003

We applied a finite-difference time domain algorithm to the study of field and intensity correlations in random media. Close to the onset of Anderson localization, we observe deviations of the correlation functions, in both shape and magnitude, from those predicted by the diffusion theory. Physical implications of the observed phenomena are discussed. © 2004 Optical Society of America

OCIS codes: 030.1670, 290.4210, 290.1990.

Light propagating in a random medium undergoes multiple scattering. As a result, it forms a complex interference (speckle) pattern when it emerges from the medium, which can be described statistically.^{1,2} There exist longer-range correlations that can be detected as correlations between two distant speckles.^{3,4} These longer-range correlations in transmitted intensities have received much attention in the context of mesoscopic electronic systems,⁵ in which they result in universal conductance fluctuations. For electronic systems, only limited information (fluctuation of conductance) can usually be deduced from experiments. For light, however, momentum-resolved (angular) and spatially resolved measurements are possible. The latter yield much more detailed information about the system. The connection between electrons and photons is established by identifying the Landauer conductance g with the total transmission coefficient (summed over all incoming and outgoing channels).⁵ The majority of experimental and theoretical efforts (see Refs. 1, 6–8 and references therein) to date have been concentrated on systems in the regime of diffusive transport, $g \gg 1$. The intensity correlation function (ICF) is defined as^{7,8}

$$C(\Delta r, \Delta \nu) = \frac{\langle I(\mathbf{r} + \Delta \mathbf{r}, \nu + \Delta \nu) I(\mathbf{r}, \nu) \rangle}{\langle I(\mathbf{r} + \Delta \mathbf{r}, \nu + \Delta \nu) \rangle \langle I(\mathbf{r}, \nu) \rangle} - 1, \quad (1)$$

where \mathbf{r} and ν are the spatial coordinate and frequency, respectively. When the random medium's length L is greater than its width W , C is invariant with respect to \mathbf{r} and isotropic⁹ for $\Delta \mathbf{r}$ as long as one avoids the evanescent zone on the output surface.¹⁰ Theoretically, based on pairing of incoming and outgoing channels, three contributions to the ICF have been identified^{3,4,7,8}: short-range C_1 , long-range C_2 , and infinite-range C_3 . Deep into diffusion regime $g \gg 1$ in a waveguide geometry^{7,8} $C_1 \approx |C_E(\Delta r, \Delta \nu)|^2 \sim 1$, $C_2 \sim 1/g$, and $C_3 \sim 1/g^2$, making the values of C_2 and C_3 small. Here

$$C_E(\Delta r, \Delta \nu) = \frac{\langle E(\mathbf{r} + \Delta \mathbf{r}, \nu + \Delta \nu) E^*(\mathbf{r}, \nu) \rangle}{\langle I(\mathbf{r} + \Delta \mathbf{r}, \nu + \Delta \nu) \rangle^{1/2} \langle I(\mathbf{r}, \nu) \rangle^{1/2}} \quad (2)$$

is the field correlation function (FCF). Essentially, the nonperturbative nature of the crossover from diffusion to localization limits the amount of information that can be obtained theoretically.¹¹ The purpose of this Letter is to introduce a numerical method for studying correlation functions (CFs) based on a finite-difference time-domain¹² algorithm. This method allows us to solve Maxwell's equations for the electromagnetic field at every spatial grid at every time step. It makes no assumption about the scattering strength, accounts for all interference phenomena, and makes it possible to obtain CFs in both diffusion and localization regimes. Here we apply our method to systems with values of g from 4.5 to 1.

We consider a two-dimensional system as shown in the inset in Fig. 1: a parallel-plate metallic waveguide filled with circular dielectric scatterers of refractive index $n = 2$ and diameter $d = 1.4$ cm. We chose our parameters to be close to the microwave experiments in Ref. 13. The scatterers were randomly positioned (without overlapping) with a fixed filling

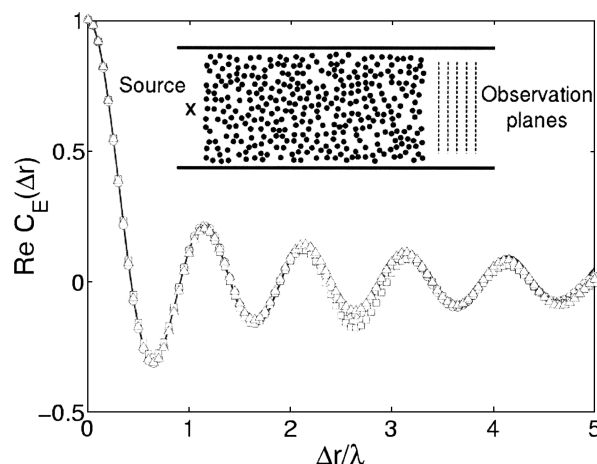


Fig. 1. Real part of spatial FCF. Squares, circles, and triangles correspond to the systems with g of 4.4, 2.2, and 1.1, respectively. The solid curve represents the fit of Eq. (3) with $z_b/l = 0.8$. The inset shows the geometry of our system.

fraction $f = 0.3$. The metallic walls of the waveguide ensured 99.9% reflectivity, and uniaxial perfectly matched layer¹² boundary conditions were applied outside the waveguide. A TM-polarized broadband pulse with a center wavelength of $\lambda = 2$ cm (close to one of the Mie resonances of the scatterers) was launched by means of a point source placed one wavelength from the left surface of the random medium inside the waveguide. A temporal discrete Fourier transform was applied to electric fields observed at a series of vertical planes separated by $\lambda/2$ at the output end of the waveguide. By virtue of the discrete Fourier transform, we obtained the continuous-wave response of the system for a number of wavelengths λ_i within a 4% range of λ . This range was significantly narrower than the width of the broadband pulse and the range in which physical parameters of the system start to deviate from those at λ . The distance between two consecutive λ_i was chosen to be equal to the average mode spacing. We obtained spatial field and intensity CFs by setting $\Delta\nu = 0$ in Eqs. (1) and (2). We averaged more than 48 configurations and 60 λ_i , which is similar to the microwave experiments in Ref. 13. In addition, because of the invariance of correlations in the empty part of the waveguide, we averaged more than ten observation planes. As many as 100 spatial points equally spaced near the center of each plane were sampled depending on Δr . For spectral CFs, obtained with Eqs. (1) and (2) with $\Delta r = 0$, the averaging procedure is similar except that the number of λ_i sampled depends on the value of $\Delta\nu$.

Waveguide geometry makes our system quasi-one-dimensional, with localization length $\xi \propto Nl$. N is the number of waveguide channels, and l is the transport mean free path. With an increase in L the system crosses over from diffusion to localization while l is kept constant. According to the diffusion theory, the dimensionless conductance of a quasi-one-dimensional system is $g = (\pi/2)n_{\text{eff}}^{(e)}Nl/L'$, where $L' = L + 2z_b$ accounts for the boundary effect,¹⁴ the extrapolation length z_b is usually of the order of l , $n_{\text{eff}}^{(e)} = c/v_E$, and v_E is the energy transport velocity.¹⁵ In a passive system g is equal to the Thouless number, which is defined as the ratio of the diffusion mode linewidth to the average mode spacing.^{6,16} In our system $l = 1.8$ cm and $n_{\text{eff}}^{(e)} = 1.77$ (see below). The width of waveguide $W = 20$ cm ($N = 2W/\lambda = 20$) and lengths L of 20, 40, and 80 cm yielded g of 4.4, 2.2, and 1.1, respectively, and allowed us to study the correlation functions near the onset of localization.

To determine z_b , the real part of the spatial FCF can be fitted with the formula

$$C_E(\Delta r) = \frac{\pi(z_b/l)J_0(k\Delta r) + 2 \sin(k\Delta r)/k\Delta r}{\pi z_b/l + 2}, \quad (3)$$

where $k = 2\pi/\lambda$, and J_0 is a Bessel function of zeroth order. The imaginary part of $C_E(\Delta r)$ should vanish due to isotropy,⁹ which is confirmed by our calculation in which its value was less than 10^{-3} . We derived the above expression in two dimensions following the three-dimensional derivation of Ref. 17. Equation (3) gives an excellent fit for all systems

studied with $z_b/l = 0.8$ in Fig. 1. Absence of the deviation of $C_E(\Delta r)$ from the expression derived in the diffusion regime becomes apparent when one recognizes that $C_E(\Delta r)$ contains only information about short-range correlations. It reflects the correlations on a length scale of l , which is much smaller than ξ . $n_{\text{eff}}^{(e)}$ in the expression for g can be calculated as $n_{\text{eff}}^{(e)} = (1 \times W_{\text{air}} + n \times W_{\text{scat}})/(W_{\text{air}} + W_{\text{scat}})$, where W_{air} and W_{scat} are the energy stored in air and scatterers, respectively. W_{air} and W_{scat} were determined numerically to give $n_{\text{eff}}^{(e)} \approx 1.77$. The physical parameter yet to be obtained is the transport mean free path l . This can be done by fitting the spectral CF to the complex function^{18,19}

$$C_E(\Delta\nu) = qL'/\sinh qL', \quad (4)$$

where $q = (\pi\Delta\nu/D)^{1/2}(1 - i)$. l enters Eq. (3) through L' , and the diffusion coefficient $D = v_E l/2$. Figure 2 shows the fitting of the real and imaginary parts of $C_E(\Delta\nu)$, from which we find $l = 1.8$ cm. The HWHM of $|C_E(\Delta\nu)|^2$ should coincide with 1.46 times the diffusion mode linewidth $\delta\nu = D/L'^2$, at least in the diffusion regime. The inset in Fig. 2 shows that the obtained l and $\delta\nu$ are consistent. A slight deviation in the system of $g = 4.4$ is attributed to its short length.

The spatial dependence of the long-range contribution to the ICF was derived in diffusion up to the $1/g^2$ order¹³:

$$C(\Delta r) - |C_E(\Delta r)|^2 = \left(\frac{4}{3g} + \frac{8}{15g^2}\right) \frac{1 + |C_E(\Delta r)|^2}{2}. \quad (5)$$

Figure 3 shows both the magnitude and the normalized profile of Eq. (5). The numerically calculated $C(\Delta r) - |C_E(\Delta r)|^2$, shown in Fig. 3, reveals that its spatial profile is independent of g . Specifically, the ratio of its value at $\Delta r = 0$ to that at $\Delta r \rightarrow \infty$ remains

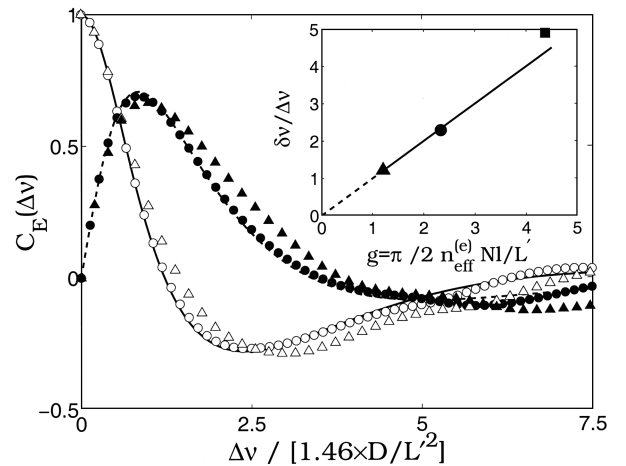


Fig. 2. Real (empty symbols) and imaginary (filled symbols) parts of the frequency FCF. Solid and dashed curves represent the real and imaginary parts, respectively, of C_E given by Eq. (4) with $l = 1.8$ cm. The inset compares $\delta\nu$ found with a HWHM of $|C_E(\Delta\nu)|^2$ to D/L'^2 . Both quantities are normalized to average mode spacing. Symbol notations are the same as in Fig. 1.

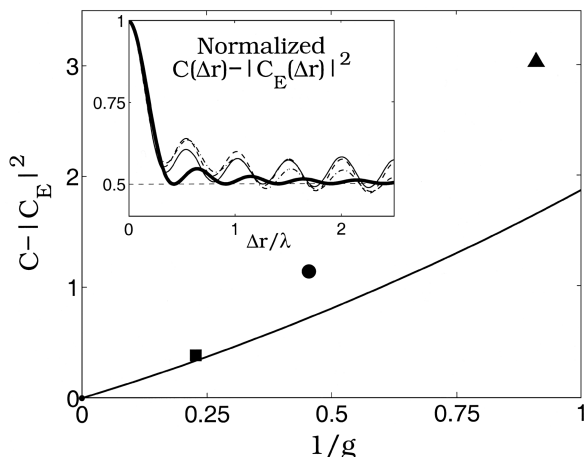


Fig. 3. Magnitude of long-range contribution to ICF versus dimensionless conductance g . Symbol notations are the same as in Fig. 1. Solid line represents diffusion expansion formula Eq. (5) at $\Delta r = 0$. The inset shows the long-range contribution to the ICF normalized to 1 at $\Delta r = 0$. Solid, dashed, and dotted-dashed curves correspond to samples with g of 4.4, 2.2, and 1.1, respectively. Thick solid curve plots Eq. (5).

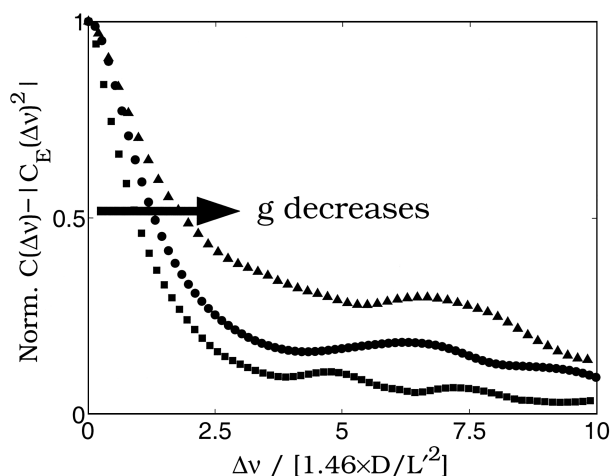


Fig. 4. Frequency dependence of the long-range contribution to the ICF normalized to value at $\Delta\nu = 0$. Symbol notations are the same as in Fig. 1.

equal to 2. Stronger oscillations in the numerical data are likely due to the finite width of the waveguide. However, the magnitude of the long-range contribution is significantly enhanced because of localization effects, far beyond the diffusion prediction up to the order of $1/g^2$.

In Fig. 4, as g decreases, the long-range contribution to spectral ICF, $C(\Delta\nu) - |C_E(\Delta\nu)|^2$, is broadened when $\Delta\nu$ is normalized to $\delta\nu$. We ascribe this effect to

strong fluctuations close to the localization threshold; namely, a few (more conducting) channels with larger than average linewidth dominate ICF, leading to its spectral broadening.

In conclusion, using the finite-difference time domain algorithm, we studied field and intensity correlation functions close to the onset of localization. In this regime neither experiments nor analytical theories have given such detailed information about the correlation of intensities transmitted through a random medium.

A. Yamilov and H. Cao are grateful to Azriel Genack and Boris Shapiro for their comments on the manuscript and fruitful discussions. This work was supported by the National Science Foundation under grant DMR-0093949. H. Cao acknowledges support from the David and Lucile Packard Foundation. A. Yamilov's e-mail address is a-yamilov@northwestern.edu.

References

1. P. Sebbah, ed., *Waves and Imaging Through Complex Media* (Kluwer Academic, Dordrecht, The Netherlands, 2001).
2. B. Shapiro, Phys. Rev. Lett. **57**, 2168 (1986).
3. S. Feng, C. Kane, P. A. Lee, and A. D. Stone, Phys. Rev. Lett. **61**, 834 (1988).
4. P. A. Mello, E. Akkermans, and B. Shapiro, Phys. Rev. Lett. **61**, 459 (1988).
5. C. W. J. Beenakker, Rev. Mod. Phys. **69**, 731 (1997).
6. P. Sheng, ed., *The Scattering and Localization of Classical Waves* (World Scientific, Singapore, 1990).
7. R. Berkovits and S. Feng, Phys. Rep. **238**, 136 (1994).
8. M. C. W. van Rossum and Th. M. Nieuwenhuizen, Rev. Mod. Phys. **71**, 313 (1999).
9. P. Sebbah, R. Pnini, and A. Z. Genack, Phys. Rev. E **62**, 7348 (2000).
10. A. Apostol and A. Dogariu, Phys. Rev. Lett. **91**, 093901 (2003).
11. A. D. Mirlin, A. Müller-Groeling, and M. R. Zirnbauer, Ann. Phys. **236**, 325 (1994).
12. A. Taflove and S. C. Hagness, *Computational Electrodynamics* (Artech House, Norwood, Mass., 2000).
13. P. Sebbah, B. Hu, A. Z. Genack, R. Pnini, and B. Shapiro, Phys. Rev. Lett. **88**, 123901 (2002).
14. A. Lagendijk, R. Vreeker, and P. de Vries, Phys. Lett. A **136**, 81 (1989).
15. M. P. van Albada, B. A. van Tiggelen, A. Lagendijk, and A. Tip, Phys. Rev. Lett. **66**, 3132 (1991).
16. A. A. Chabanov, M. Stoytchev, and A. Z. Genack, Nature **404**, 850 (2000).
17. I. Freund and D. Eliyahu, Phys. Rev. A **45**, 6133 (1992).
18. N. Garcia and A. Z. Genack, Phys. Rev. Lett. **63**, 1678 (1989).
19. M. C. W. van Rossum and Th. M. Nieuwenhuizen, Phys. Lett. A **177**, 452 (1993).